

Article

Hydrochemical Characteristics and Quality Evaluation of Irrigation and Drinking Water in Bangong Co Lake Watershed in Northwest Tibetan Plateau

Yuxiang Shao ¹ , Buqing Yan ^{1,*}, Lubaiyang Liu ², Xiao Yu ¹, Gang Feng ¹, Kun Zhang ¹ and Kang Gong ¹

¹ Research Center of Applied Geology of China Geological Survey, Chengdu 610036, China; shaoyuxiangcgs@outlook.com (Y.S.); jiazhuo@126.com (X.Y.); fg17716159968@163.com (G.F.); 18683651975@163.com (K.Z.); 17608058483@163.com (K.G.)

² Xi'an Institute for Innovative Earth Environment Research, Xi'an 710061, China; liuyang@ieecas.cn

* Correspondence: 127961917@139.com

Abstract: Bangong Lake is a narrow and long lake in the arid region of the plateau in northern Tibet. The salinity of the east of the lake is different from that the west, resulting in differences in the natural environment and human living conditions on each side. Watershed hydrochemical analysis and spatial statistical analysis can help to understand regional hydrochemical evolution and water quality evaluation. In this study, the hydrochemical characteristics of surface water (glacier, river, and lake) and groundwater in the Bangong Co Lake Watershed were investigated to reveal the relationships between various water bodies. The drinking water quality index (DWQI) and USSL classification were applied to assess groundwater quality suitability for agricultural and drinking purposes. The hydrochemical characteristics show the differences among water bodies and their spatial distribution. The analyzed groundwater and surface water samples, such as river water and glaciers, were mainly Ca-HCO₃-type and the lake water was mainly categorized as Na-Cl-type with some Na-HCO₃-Cl type. The lake water's chemical components are mainly affected by evaporative karst decomposition. The main mineralization process of groundwater and river water was related to the dissolution of reservoir minerals, such as dolomite and calcite, as well as halite. The drinking water quality index (DWQI) indicates that 79% of the groundwater samples in the study area were of good enough quality for drinking. In terms of irrigation water quality, the electrical conductivity (EC), calculated sodium adsorption ratio (SAR), and magnesium hazardous ratio (MHR) showed that more than 13% of the total samples were not suitable for irrigation. However, the USSL classification indicated that glacier and river water are relatively suitable for irrigation. Additionally, some groundwater and lake water has very high alkalinity or salinity, which is alarming when considering them for irrigation.

Keywords: Bangong Co Lake Watershed; hydrochemical characteristics; water quality; surface water; groundwater



Citation: Shao, Y.; Yan, B.; Liu, L.; Yu, X.; Feng, G.; Zhang, K.; Gong, K. Hydrochemical Characteristics and Quality Evaluation of Irrigation and Drinking Water in Bangong Co Lake Watershed in Northwest Tibetan Plateau. *Water* **2023**, *15*, 2655.

<https://doi.org/10.3390/w15142655>

Academic Editors: Ahmed Elbeltagi, Quanhua Hou and Bin He

Received: 28 June 2023

Revised: 16 July 2023

Accepted: 19 July 2023

Published: 22 July 2023



Copyright: © 2023 by the authors. Licensee MDPI, Basel, Switzerland. This article is an open access article distributed under the terms and conditions of the Creative Commons Attribution (CC BY) license (<https://creativecommons.org/licenses/by/4.0/>).

1. Introduction

The Tibetan Plateau, known as the roof of the world and the water tower of Asia, is the birthplace of the Yellow River, the Yangtze River, the Ganges River, the Mekong River, the Indus River, and other rivers, and has the largest, highest, and most densely distributed alpine lake cluster in the world [1,2]. In the Tibetan Plateau, lakes play an important role in regulating the ecosystem and hydrochemistry and are a vital indicator of water-rock interaction and environmental change in the basins [3,4]. In the last few years, many academics have conducted investigations on lakes in the Tibetan Plateau, which mainly focused on hydrochemical characteristics and its spatial distribution [5,6], typical water pollutants [7], water quality assessment [8,9], and hydrochemistry evolution and sources [10,11]. Due to the vulnerability of the water environment to climate change

and the scarcity of water resources in the alpine desert, water quality assessment and hydrochemical evolution in these areas have attracted increasing attention [12,13].

Natural factors, such as the geological structure, hydrogeological conditions, vegetation, climate, rock weathering, terrain, and human activities, greatly impact the chemical composition of water [14]. Sun and Jin pointed out the differences in chemical characteristics and evolution between tectonic and glacial lakes on the plateau based on the analysis of physicochemical parameters and ion concentrations of lakes in the Tibetan Plateau [6]. Li et al. discussed the relationship between lake change and climate in recent decades and clarified that lakes are important supporters of the water cycle and environmental change [15]. Based on spatial analysis of the heavy metal contents in ores, air pollutants, and lake water samples, Bazova and Moiseenko discussed the sources of heavy metals in lakes in northwestern Russia, and the results showed that the concentration of Cu, Ni, Mn, Zn, Pb, and As in lake water was caused by anthropogenic pollution, such as flue gas emissions of metallurgical enterprises [16]. Baranov et al. studied the chemical composition, natural geochemistry, and human factors of dissolved effluents in the northern Valdai Mountains using statistical methods [17]. The results showed that the soil mineral composition, rainfall intensity, and biogeochemical processes had a great influence on the chemical composition of water bodies in the aeration zone. Moreover, many scholars have gained a significant understanding of regional soil salinization, regional geological background, element migration and enrichment law, petrophysical weathering process, and other aspects by studying ion characteristics of watershed water bodies [18]. It can be seen that the hydrochemical characteristics of natural water bodies are one of the important indicators when studying regional water cycles and evolution.

The reserves and quality of water resources are important for the stable and sustainable development of human society and natural ecology. Good water quality is especially valuable in water shortage areas. High evaporation and low rainfall lead to salinization or heavy metal pollution in shallow groundwater or surface water in lake basins in the arid region of the plateau [19]. Previously, water quality assessments were carried out on many lake basins in the Tibetan Plateau, such as Qinghai Lake [20], the Ebinur Lake Watershed [21], Dal Lake in Kashmir Valley [22], Mapam Yumco [23], and Nam Co [24]. The results showed that the water quality of most lakes was relatively uniform and fluctuated in a small range. The results also indicated that lake water with high salinity had a great influence on the shallow surface water of the lake shore, and the salinity of groundwater had a great influence on plant growth, human life, animal husbandry development, and industrial activities in the region.

Bangong Co Lake is a long and narrow tectonic lake with a nearly east–west distribution. The western part of the Tibetan Plateau is characterized by a dry and cold climate with strong evaporation [25]. As the main source of replenishment for the Lake Bangong Co Watershed, glacial meltwater is insufficient to balance evaporation in the area. Likewise, affected by evaporation across the whole watershed and river water supply in the east of Bangong Co Lake, the salinity of the lake gradually increases from east to west [26]. The water circulation system of the plateau arid watershed is very fragile and sensitive, which makes the water resources in the study area vulnerable to the impacts of human activities, animal husbandry activities, and climate change.

Some scholars investigating lake groups on the Tibetan Plateau have pointed out that the lake water type on the east side of Bangong Co Lake is Cl-Na or $\text{HCO}_3\text{-Cl-Mg}\cdot\text{Na}$ [27,28]. Lin et al. researched information on toxic organic pollutants and metals of Bangong Co Lake, and their results indicate that polycyclic aromatic hydrocarbons (ΣPAH) and phthalic acid esters (ΣPAE) concentrations in lake water have no relationship with hydrochemical parameters, and organic pollutants have been the main source of domestic waste related to increasing regional human activities in recent years [29]. The domestic water and irrigation water in the study area are mainly shallow aquifers in the lakeshore zone and river valley or supplemented by snowmelt water and river water. However, there are few relevant studies on the various water bodies of Bangong Co Lake Watershed. Therefore, the hydrochemical

characteristics and controlling factors of the river water, lake water, groundwater, and other water bodies in the watershed of Bangong Co Lake are still unknown. Additionally, there is no available information on water quality assessment in this region.

The present investigation was performed to explore the glaciers, rivers, lakes, and groundwater along the lakeshore in the Bangong Co Lake Watershed. Statistical analysis, a Gibbs diagram, a Piper diagram, and an ion ratio analysis were used to analyze the hydrochemical characteristics and formation mechanisms of different water bodies. The drinking water quality index (DWQI) and irrigation water quality parameters were used to assess the water quality and its suitability in the study area. The specific objectives of this work are as follows: (i) To explain the hydrochemistry and evolution of different water bodies in Bangong Lake Basin, (ii) to identify the various factors controlling the water chemistry in this area, and (iii) to assess the suitability of the water quality for drinking and irrigation.

2. Materials and Methods

2.1. Study Area

Bangong Co Lake Watershed is located in the northwest of Tibet, China. Based on ArcGIS hydrological analysis module and DEM data, the watershed area of Bangong Co Lake is about 33,000 km², with the location between 32°40′–34°30′ N and 78°10′–81°15′ E, with an elevation range of 3736–6771 m. The watershed reaches the Kanakoram Mountains in the north and the Gangdise Mountains in the south. The highest point is located in the eastern mountains of Zecuo Lake, and the lowest is located in Bangong Co Lake, in the middle of the area (Figures 1 and 2). The geomorphology of the watershed is that of plateau lake basin geomorphic type, which has been fully eroded by snow and water for a long time. The watershed covers the Bangong Lake replenishment river basin and several small intermountain lake basins, such as Spangour Co, Zecuo, Rebangcuo, Aiyongcuo, and Sharda Co [30]. This region has a cold and dry climate, with an average annual temperature of 0.1–2 °C. The annual rainfall is about 70–80 mm, with high variability, and is mostly concentrated in July or August [31]. The main source of water in the study area is glacial meltwater. Due to gravity, the water mainly flows along the slope or gully to feed rivers or veins of rock and eventually drains into the lake. Because the sediments in river valleys in the middle or lower reaches and the sediments in lake shores are thick and loose, the river water is likely to penetrate, forming relatively stable shallow groundwater in the alluvial fan or valley area.

Geologically, the study area is located in the nearly east–west Bangong Co–Nujiang suture zone, with Qiangtang block to the north and Lhasa block to the south (Figure 1) [32,33]. Qiangtang block in the region is mainly composed of carbonate rocks, sandstone, and slate rocks from Yanshiping formation, Tunlonggongba formation, and Nuoco formation, and Lhasa Terrane in the study area is mainly composed of ophiolite mélangé, Cretaceous gabbros and granites, and sandwiched limestone and flysch sediments from Mugangan-gri Group and Langshan formation (Figure 1) [31,34]. Quaternary sediments are mainly distributed on the sides of lake and river valleys. NWW-trending and NE-trending faults are mainly developed in the Bangong Co Lake area. Most faults align with the boundary of the lake basin in geomorphology, and the fault surface is shovel-type dip into the lake. Meanwhile, the NWW-trending faults are the leading faults in the region, belonging to the Bangong Co–Nujiang suture system, which has undergone multiple periods of subduction, collision, and other tectonic processes, and are nearly consistent with the overall tectonic line and the ophiolitic hybrid zone. The NE-trending faults are mostly developed in some north–south gullies and valleys and have the characteristics of water conduction after differentiation and denudation [35].

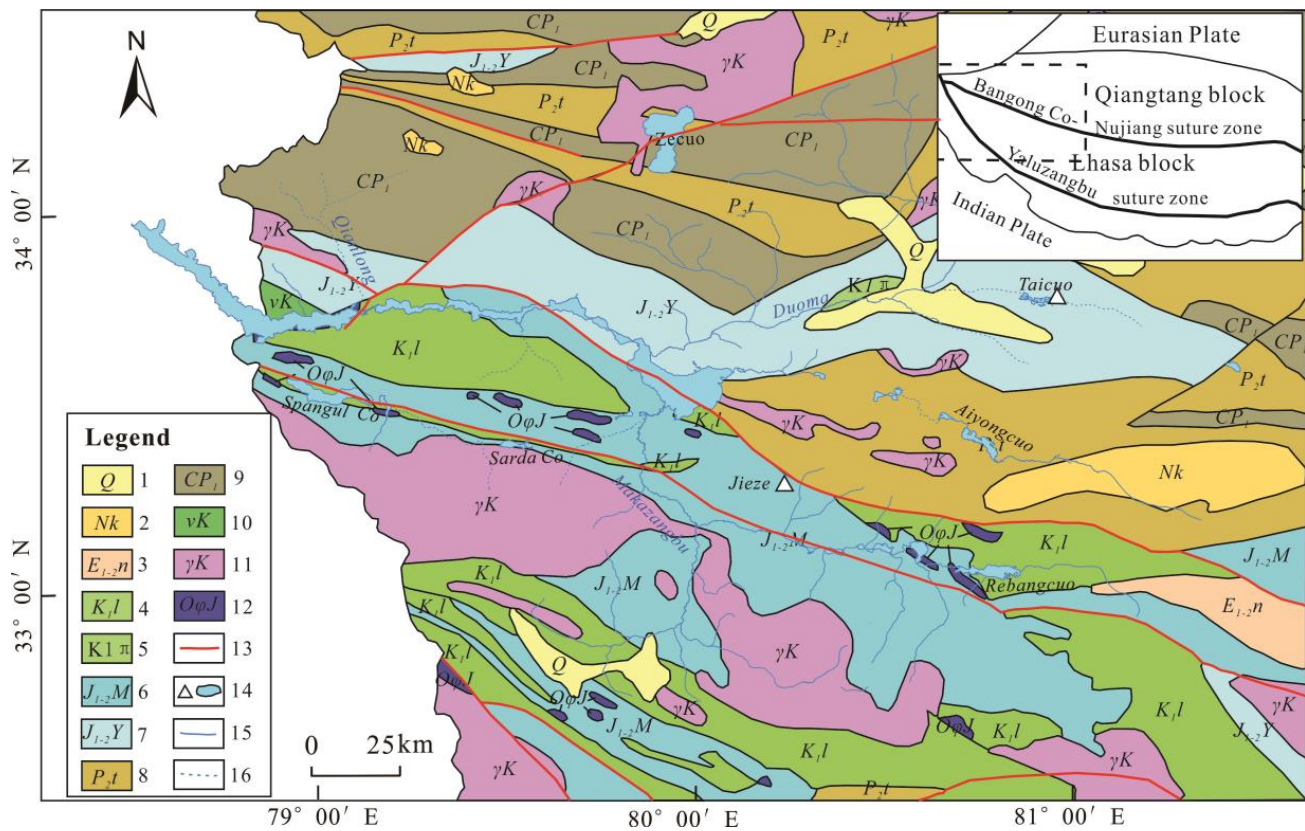


Figure 1. 1: Quaternary. 2: Sandstone and conglomerate of Cantuo Fm. 3: Mudstone and conglomerate of Niubao Fm. 4: Limestone of Langshan Fm. 5: Limestone and sandstone of Tielongtan Gr. 6: Argillaceous slate and metamorphic sandstone of Mugagangri Gr. 7: Limestone and clastic rocks of Yanshiping Gr. 8: Sand shale and limestone of Tunlonggongba Fm. 9: Silty slate of Nuoco Fm. 10: Cretaceous gabbro. 11: Cretaceous granite. 12: Ophiolite. 13: Faults. 14: Salt lake (salt mine) and lake. 15: Perennial river. 16: Seasonal river. (this figure is modified from the regional geological map released by the GeoCloud Platform of the China Geological Survey).

There are many aquatic plants and fishes in Bangong Co Lake. Fishes mainly include Schizothoracinae and *Triplophysa stenura*, and the aquatic plants encompass Pyrrophyta, Bacillariophyta, and Chlorophyta [28]. Moreover, a small field of wetlands lies east and southeast of the lake, mainly growing plateau meadows and reeds. Plateau desert meadow is the main vegetation type in the Bangong Co Lake catchment area. The dry period is a maximum of nine months in this area, so the grass yield of the regional meadow is relatively low [36]. Animal husbandry activities are mainly concentrated in the rainy season, and animal husbandry activities are basically practiced in areas with abundant groundwater, such as alluvial fan front, lakeshore, and valley land.

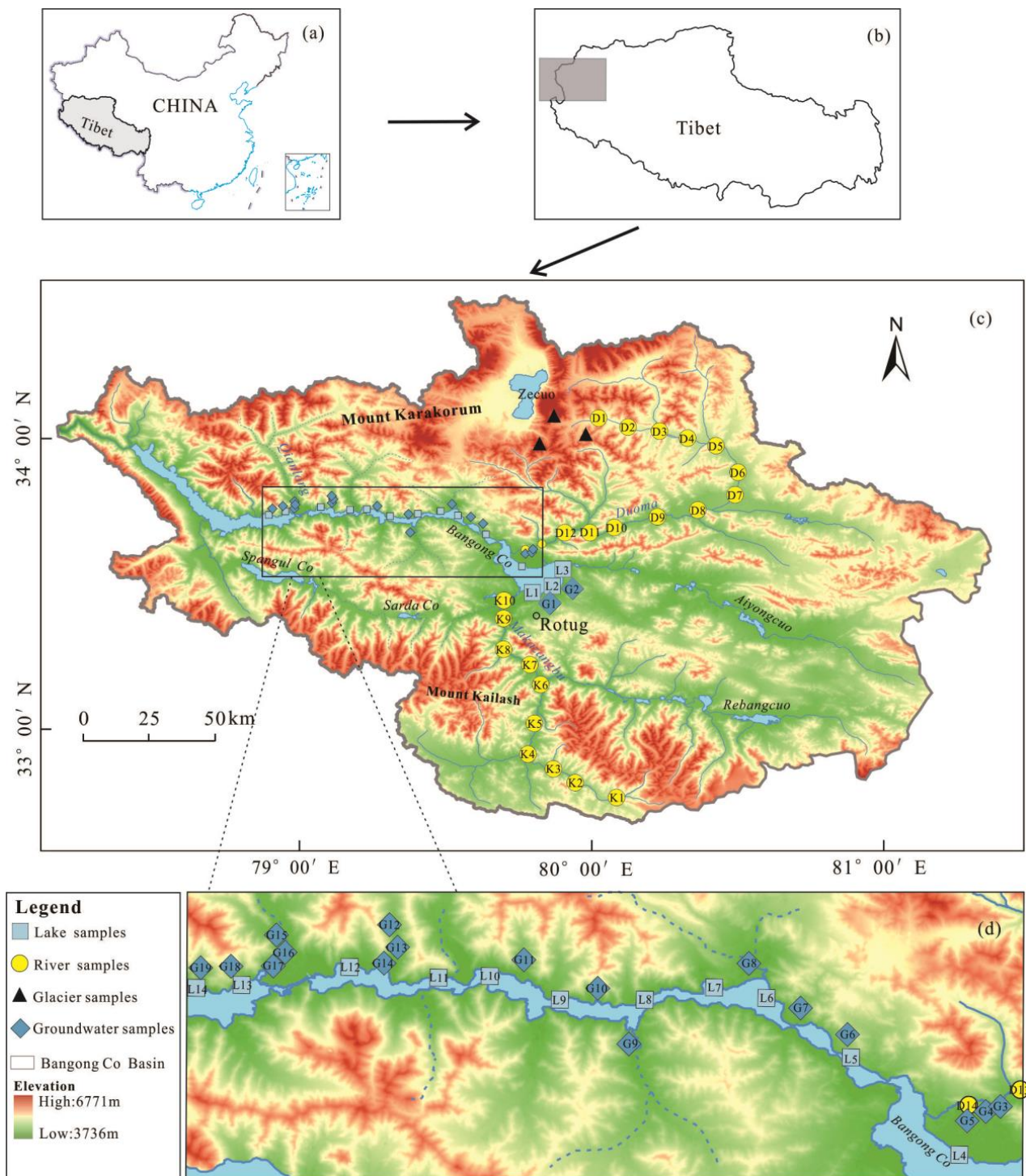


Figure 2. (a) The location of the Tibet Autonomous Region in China; (b) a map of the study area; (c,d) geomorphology of sampling sites and study areas.

2.2. Sampling and Measurement

In early June 2022, field investigation was carried out in Bangong Lake Basin, and a total of 60 water samples were collected, including 14 lake water samples, 19 groundwater samples, 24 river water samples, and 3 glacier water samples (Figure 2). Among them, river samples were mainly distributed in Makazangbu and Doma Rivers, and groundwater samples were mainly collected from wells on alluvial fan bodies in lakeshore zone. The water depth of the collected wells was less than 15 m, and most of the glacier samples were

new snow samples. Water samples were mostly collected at a depth of 0.1–0.5 m, filtered through 0.45 μm cellulose acetate membrane, and stored in 1500 mL cleaned polyethylene bottles. Before collection, the collection containers were rinsed with sampling water 2 to 3 times. The lake water samples were taken from a location about 1–2 m away from the lake. In addition, water electrical conductivity (EC) and pH were measured in the field using a multi-parameter portable water analyzer (Manta, Eureka Inc., Austin, TX, USA), with a pH accuracy of ± 0.1 pH and conductivity accuracy of ± 1 $\mu\text{S}/\text{cm}$.

All collected samples were stored in 0–4 $^{\circ}\text{C}$ incubators until they were analyzed in the laboratory. Parallel samples were used to control the test's accuracy during the experiment. For any water sample, a part of it was acidified with 1:1 nitric acid and stored in a plastic bottle for cation analysis. The remaining part was placed in glass bottles and sealed with parafilm sealing film to analyze anions such as SO_4^{2-} and Cl^- . The content of HCO_3^- was measured by acid–base titration, with an accuracy of $\pm 0.05\%$. Water salinity (TDS) was determined using the dry weight method at 105 $^{\circ}\text{C}$, with an accuracy of $\pm 0.2\%$. Total hardness (TH) was determined using the EDTA method with an accuracy of $\pm 0.05\%$. The main cation (Na^+ , K^+ , Ca^{2+} , and Mg^{2+}) concentrations and trace heavy metal (Fe, Mn, Zn, Cu, and Cr) levels were determined using inductively coupled plasma emission spectrometer (Agilent5110, Agilent Technologies Inc., Santa Clara, CA, USA), and the testing error was less than 2%. The total As content was detected via atomic fluorescence (AFS-933, Beijing Jitian Instrument Co., LTD, Beijing, China) with an accuracy of $\pm 0.5\%$. Anion concentration (SO_4^{2-} , Cl^- , F^- , and NO_3^-) was determined via chromatography (ECO IC, Vantone China Co., LTD, Beijing, China), and the testing error was less than 0.5%. The ion balance of the major soluble cationic equivalent ($\text{TZ}^+ = \text{Na}^+ + \text{K}^+ + 2\text{Ca}^{2+} + 2\text{Mg}^{2+}$) and soluble anionic equivalent ($\text{TZ}^- = \text{Cl}^- + \text{NO}_3^- + \text{HCO}_3^- + \text{F}^- + 2\text{SO}_4^{2-}$) of all samples was compared for ion balance test, and it was within $\pm 5\%$. All water samples were finished by Xizang Shengyuan Environmental Engineering Co., LTD, Tibet, China.

2.3. Data Processing

SPSS v22.0 (SPSS Inc., Chicago, IL, USA) was used to determine the average (Mean), maximum (Max), minimum (Min), and coefficient of variation (CV). The Piper diagrams [37], principal component analysis, Gibbs diagrams [38], and ion ratio analysis [39] were implemented in Origin v2021 (OriginLab, Northampton, MA, USA) and Microsoft Excel v2013 (Microsoft Corp., Redmond, WA, USA) to explore the classification and main controlling factors of the nature water in Lake Bangong Co Watershed. International standards [40], drinking water quality index [41,42], USSL classification [43], and other irrigation water indicators were used to evaluate groundwater suitability for drinking and irrigation. ArcGIS v10.4 (Esri Inc., Redlands, CA, USA) and CorelDRAW Graphics Suite v18 (Corel Corp., Ottawa, ON, Canada) were used for mapping and modification.

3. Results and Discussion

3.1. Chemical Composition of Different Water Bodies in Bangong Lake Basin

3.1.1. Statistical Characteristics of Parameters

The parameters of each water body in Bangong Co Watershed are shown in Table 1. The pH of glaciers, lake water, river water, and shallow groundwater along the lakeshore in the study area ranged from 6.6 to 8.5. The pH of glaciers was relatively low (pH = 6.6–7.6), with an average value of 7.2, which is neutral. Other water bodies were weakly alkaline as a whole, among which the pH of Bangong Co Lake water was relatively high (pH = 8.1–8.5), with an average value of 8.4. The coefficient of variation (CV) for the water pH of each water body was $<10\%$, which showed weak variability. Salinity (TDS) and electrical conductivity (EC) are parameters that can be used to determine the salinity of water [44]. The salinity (TDS) of glaciers, river water, groundwater, and lake samples ranged from 13 to 25, 81 to 438, 124 to 972, and 206 to 4091 mg/L, respectively. The salinity (TDS) values of 10 lake samples, mainly distributed in the western or middle part of the lake, exceeded the WHO's standard limit (1 g/L) [40]. The average salinity (TDS) of river

water was 282 mg/L, which was also higher than the global average and values for other large rivers in China [45]. Similarly, the electrical conductivity (EC) of glacier water, river water, groundwater, and lake samples ranged from 23 to 43, 145 to 779, 220 to 1706, and 385 to 7861 $\mu\text{S}/\text{cm}$, respectively. Water hardness is a very important parameter in the growth and reproduction of aquatic organisms [46]. The total hardness (TH) of the glaciers, groundwater, river, and lake were in the range of 23–43 mg/L, 27–750 mg/L, 58–467 mg/L, and 258–2854 mg/L, respectively. With the decrease in altitude, the values regarding the total hardness (TH), electrical conductivity (EC), and salinity (TDS) increased gradually, which were the highest around Bangong Co Lake. The coefficient of variation (CV%) for total hardness (TH), electrical conductivity (EC), and salinity (TDS) of different water bodies were between 10% and 66%, which demonstrates medium variability. Based on the total hardness (TH) and salinity (TDS) [47], lake water is hard-brackish water, glacier water is soft-fresh water, and river water changes from soft-fresh water to hard-fresh water along the stream (Figure 3).

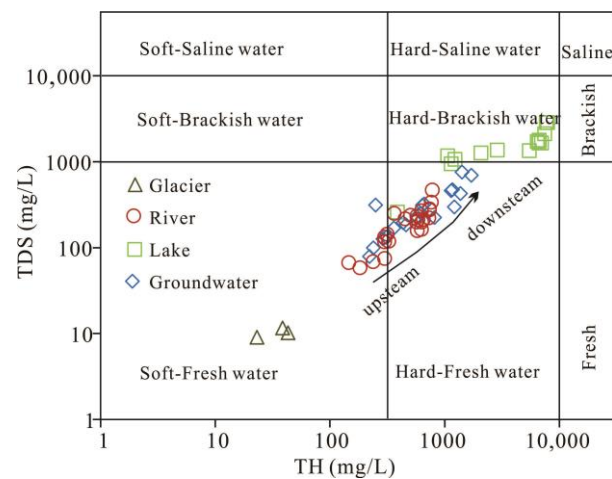


Figure 3. Classification of water in Bangong Co Lake Watershed based on total hardness (TH) and salinity (TDS).

3.1.2. Ion Spatial Distribution

The ion diagrams (Figure 4) depict the milligram equivalent and spatial variation in anions and cations in the different water bodies across the basin. In the water samples of groundwater, river water, and glaciers, the cations were dominated by Ca^{2+} , and the order of abundance was $\text{Ca}^{2+} > \text{Na}^+ > \text{K}^+ > \text{Mg}^{2+}$. However, Na^+ was the main cation of lake water, and the cation content followed the order $\text{Na}^+ > \text{Mg}^{2+} > \text{K}^+ > \text{Ca}^{2+}$. The major anion in groundwater, river water, and glacier samples was HCO_3^- , and the order of the abundance in these samples was $\text{HCO}_3^- > \text{SO}_4^{2-} > \text{Cl}^- > \text{NO}_3^-$, whereas the primary anion in lake samples was Cl^- , and the anion content followed the order $\text{Cl}^- > \text{HCO}_3^- > \text{SO}_4^{2-} > \text{NO}_3^-$. A strong coefficient of variation was found in Na^+ , Cl^- , and SO_4^{2-} of groundwater, and NO_3^- of river and lake water, which was between 1.15 and 2.85, indicating that the spatial distribution of these ionic components was unstable. The coefficient of variation of most chemical parameters of different water bodies in the area was less than 1 (Table 1), which is a weak or medium variation. Spatially, the Doma River and Maka Zangbo River showed a gradually increasing trend of ions from upstream to downstream. The main ions concentration in the lake increased gradually from east to west (Figure 4c). However, for lake samples L7 to L5 (Figures 2 and 4c), the ions and salinity (TDS) increased slowly compared to the other sections, which may be due to a water exchange barrier caused by the narrow body of the lake [50]. According to Figure 4d, there is no obvious spatial rule of groundwater in the lakeshore zone.

Table 1. Major ions and heavy metal compositions of water samples from the Bangong Co Lake Watershed.

Sample Type		pH	TDS	TH	EC	K ⁺	Na ⁺	Ca ²⁺	Mg ²⁺	Cl ⁻	SO ₄ ²⁻	HCO ₃ ⁻	NO ₃ ⁻	F ⁻	Fe	Mn	As
Glacier (n = 3)	min	6.6	13	9	23	0.15	0.25	3.08	0.22	1.04	1.96	6.67	0.18	ND	ND	ND	ND
	max	7.6	25	12	43	0.26	0.66	3.66	0.58	1.25	2.83	8.00	0.64	ND	ND	ND	ND
	Ave	7.2	20	10	35	0.20	0.49	3.44	0.36	1.12	2.38	7.56	0.35	-	-	-	-
	CV	6	27	10	24	24	36	7	43	8	15	8	60	-	-	-	-
River water (n = 24)	min	7.1	81	58	145	0.41	1.41	10.40	3.23	1.76	7.63	52.20	ND	ND	ND	ND	ND
	max	8.5	438	467	779	6.31	65.60	88.50	52.06	50.60	132.62	427.50	63.83	0.7	0.138	0.398	0.011
	Ave	7.8	282	196	498	2.28	26.98	39.93	19.89	27.65	31.89	211.56	7.68	0.2	0.044	0.115	0.005
	CV	5	39	47	39	52	61	50	54	54	90	47	213	87	82	143	68
Lake water (n = 14)	min	8.1	406	258	385	1.88	46.30	6.91	14.60	3.35	38.50	168.0	ND	ND	ND	ND	0.002
	max	8.5	4491	2854	7861	83.10	1089.0	39.80	266.40	1163.60	1004.00	1092.0	1.02	ND	0.091	0.010	0.044
	Ave	8.4	2606	1573	4546	37.85	638.31	15.84	134.06	618.50	605.25	700.64	0.10	-	0.043	0.003	0.020
	CV	1	62	43	61	73	68	56	58	69	65	52	278	-	60	76	63
Groundwater (n = 19)	min	6.8	124	79	220	0.94	3.10	12.33	7.43	3.40	0.33	66.50	1.09	ND	ND	ND	ND
	max	8.4	972	754	1706	23.44	184.0	180.00	93.50	256.00	528.00	581.70	68.57	1.5	0.224	0.441	0.003
	Ave	7.7	414	302	729	5.79	45.75	66.79	32.98	49.52	92.43	287.19	28.83	0.5	0.060	0.127	0.002
	CV	5	63	61	62	94	96	75	70	132	134	53	68	90	124	117	16
Jieze salt lake [48]		-	-	-	-	18,149	89,232	115	28,961	142,324	127,351	4054	-	-	-	-	-
Taicuo salt lake [49]		-	-	-	-	95 ± 37	1563 ± 887	1.6 ± 1.3	133 ± 12	1773 ± 653	628 ± 227	805 ± 413	-	-	-	-	-
WHO limit [40]		-	1000	500	-	-	200	-	-	250	250	-	50	1.5	0.3	0.1	0.01

The units for ion concentration are mg/L, for EC, $\mu\text{s}/\text{cm}$, and for TDS, mg/L. CV coefficient of variation, %. ND not detected.

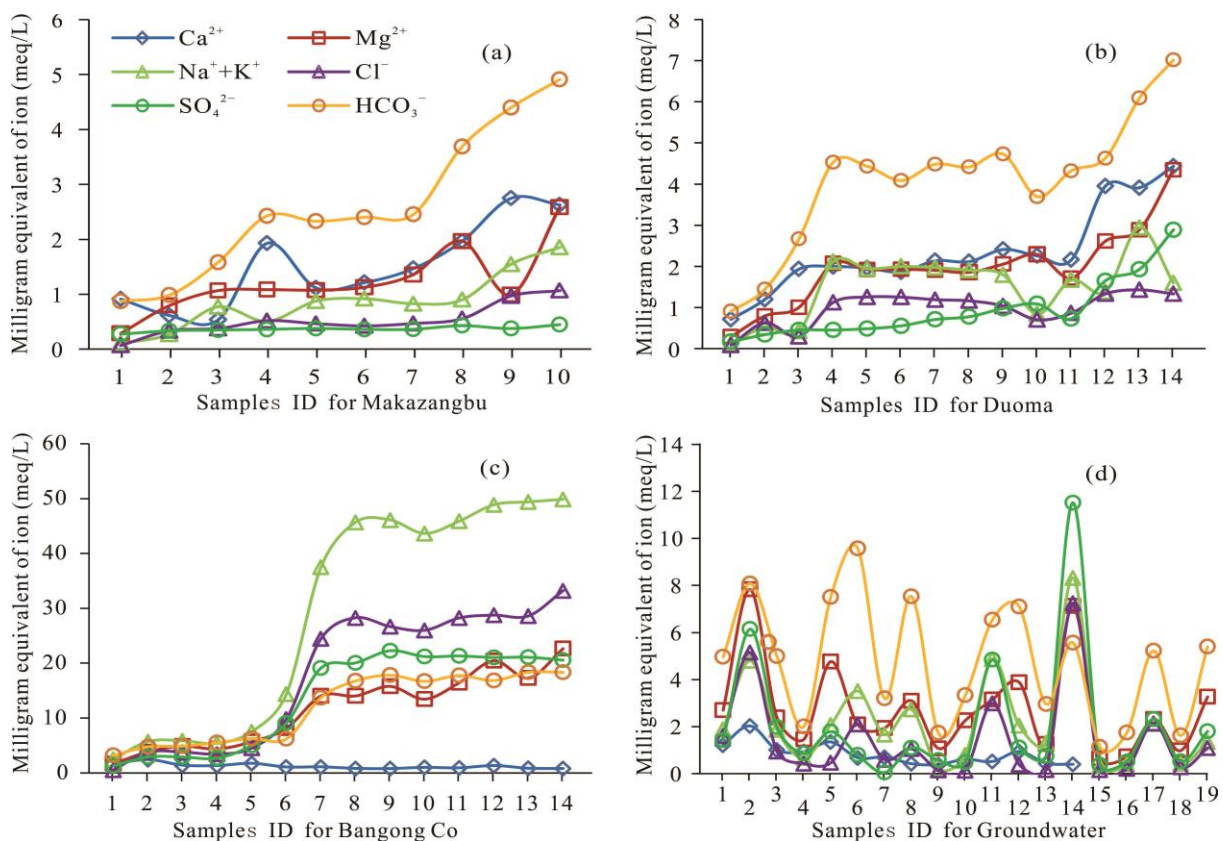


Figure 4. The spatial distribution of anions and cations in different water samples.

Al, Cr, Pb, Cd, Hg, Cu, and Ni were below the limit of quantification. Moreover, Fe, Mn, As, and F^- were found at very insignificant concentrations. Table 1 shows the summary of the datasets of trace metals. Concentrations of Fe in various water bodies varied from ND to 0.224 mg/L, which was within the WHO's tolerable limit (0.3 mg/L). Meanwhile, concentrations of As in lake samples varied from 0.002 to 0.035 mg/L, with a mean concentration of 0.021 ± 0.012 mg/L, most of which exceeded the WHO's tolerable limits (0.01 mg/L). The results were similar to those of previous studies, which suggested that the As in Bangong Co Lake was mainly derived from natural sources such as rock weathering [29]. Mn concentrations in the river and groundwater ranged from ND to 0.398 mg/L and ND to 0.441 mg/L. 4.2% ($n = 1$) in river water samples and 15.8% ($n = 3$) in shallow groundwater, exceeding the WHO's limit for Mn content (0.1 mg/L). However, few lake water samples had Mn content exceeding the WHO's standard. The Mn exceedance points of groundwater are located near the shoreline of the lake, with the pH ranging from 6.83 to 7.72. The river water exceedance point is located at a spring recharge in the lower Doma River, and the pH is 7.19. Low water pH provides favorable conditions for Mn enrichment in groundwater. On the contrary, Mn and Fe ions easily form hydroxide precipitation in lake water with relatively high pH (8.06–8.52). The flu-lacustrine purplish neogene conglomerates, rich in Fe, Mn, and other elements, are scattered in some river valleys in the study area, which may provide Mn sources for moderate and acidic groundwater. F^- concentrations of various water bodies were all below the acceptable limit according to WHO standards.

3.1.3. Piper Diagram and Hydrochemical Classification

Water hydrochemical characteristics can be classified using the Piper diagram, which shows scatter plots of cations (Na^+ , K^+ , Ca^{2+} , and Mg^{2+}) and anions (HCO_3^- , Cl^- , and SO_4^{2-}) [37,42]. According to Figure 5, water samples in the Bangong Co Lake Watershed were classified into three water types. River samples, glaciers, and most of the groundwater

corresponded to zone 2 of the Piper diagram, characterized as Ca-HCO₃-type samples. The lake samples were distributed in zone 5, classified as saline water with high Cl⁻ or SO₄²⁻ and Na⁺. Due to Cl⁻ being the main cation of lake samples, lake water was classified as a Na-Cl-type sample. Only a few groundwater samples corresponded to zone 3, representing contaminated water with high Cl⁻ and Ca²⁺ concentrations. Eastern water samples were in the transition between the river point and the lake point, indicating that these water samples exhibit ion exchange and simple dissolution or mixing.

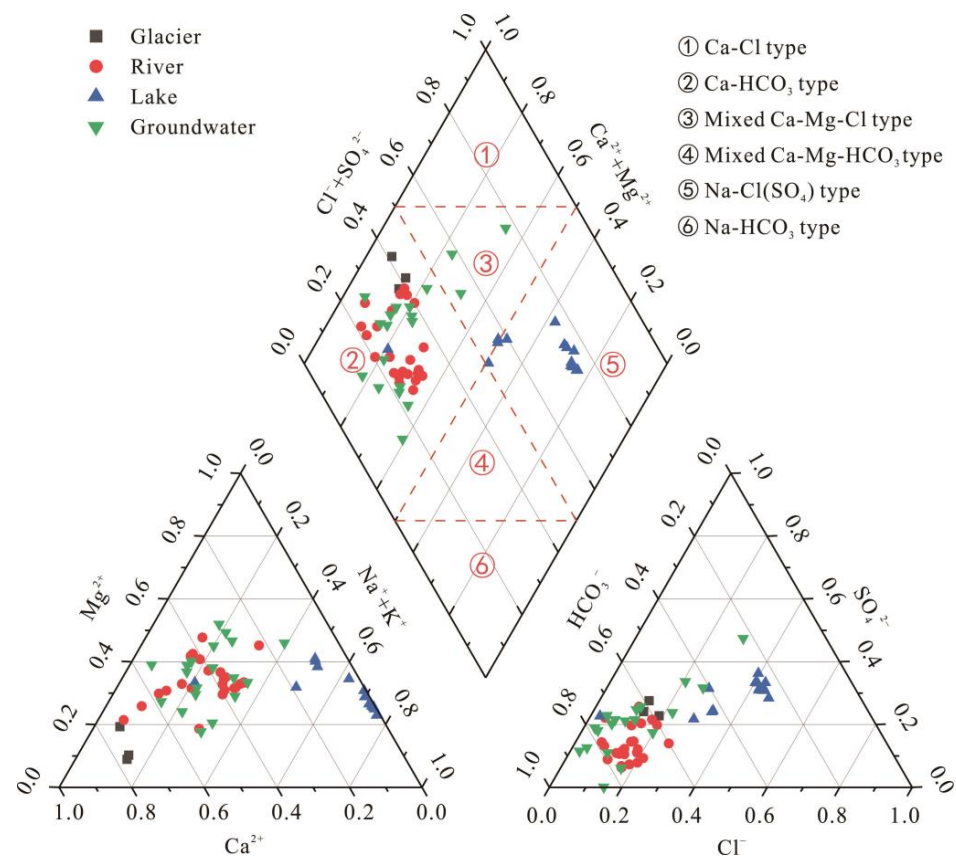


Figure 5. Piper plot of water samples in the study area.

3.2. Cause Analysis of Hydrochemical Characteristics

3.2.1. Gibbs Diagrams

Based on an analysis of many global hydrochemical compositions of surface waters, such as large lakes, rivers, and precipitation water samples, diagrams were proposed by Gibbs to determine the features of ionic distribution in different natural water bodies [38]. Rock weathering, atmospheric precipitation, and evaporation–crystallization process were identified as three major factors controlling the surface water chemistry in Gibbs plots [11,51]. In this paper, a TDS- $\text{Na}^+ / (\text{Na}^+ + \text{Ca}^{2+})$ diagram and TDS- $\text{Cl}^- / (\text{Cl}^- + \text{HCO}_3^-)$ diagram were used to distinguish the ionic characteristics of water bodies in the Bangong Co Lake Watershed (Figure 6).

With regard to the river and groundwater samples, the cation ratios $\text{Na}^+ / (\text{Na}^+ + \text{Ca}^{2+})$ varied from 0.07 to 0.66, and the anion ratios $\text{Cl}^- / (\text{Cl}^- + \text{HCO}_3^-)$ ranged from 0.02 to 0.43. Additionally, all the samples for both diagrams fell in the rock weathering domain. For the lake water samples, the ranges of the cation ratios $\text{Na}^+ / (\text{Na}^+ + \text{Ca}^{2+})$ and the anion ratios $\text{Cl}^- / (\text{Cl}^- + \text{HCO}_3^-)$ were 0.66–0.99 and 0.02–0.52, respectively. The western lake samples mainly fell into the evaporation domain (Figure 6c) or near the evaporation dominance zone (Figure 6b), and the eastern lake samples fell in the transition zone between evaporation and rock weathering (Figure 6b,c). This indicates that the dominant ions of various water bodies were significantly affected by rock weathering and evaporation–crystallization may

affect the western lake water and some groundwater. Duoma and Makazangbu rivers which were the main sources of replenishment, joined Bangong Co Lake on the east side, resulting in a characteristic transition between evaporation and rock weathering in the eastern lake. Glacier water is considered to be a precipitation sample in the Bangong Co Lake area. The glacier water samples are part of the end element of rock weathering and are slightly closer to the rain zone in Gibbs diagrams. Therefore, the dissolved ions in the rainwater of the Bangong Co Lake Watershed are slightly affected by ocean evaporation and are mainly controlled by the dissolution of atmospheric CaCO_3 particles.

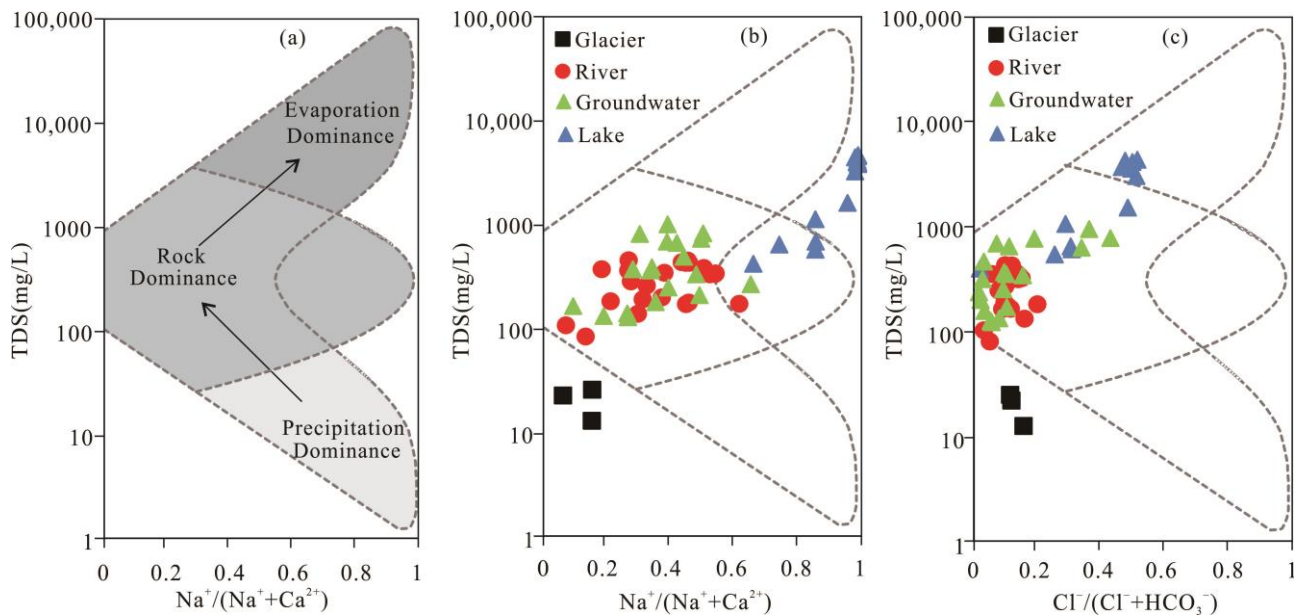


Figure 6. Gibbs plot: (a) Comparison of natural processes that define the water chemistry of water on the Gibbs (1970) diagram; (b) TDS versus $\text{Na}^+ / (\text{Na}^+ + \text{Ca}^{2+})$; (c) TDS versus $\text{Cl}^- / (\text{Cl}^- + \text{HCO}_3^-)$.

3.2.2. Ion Ratio Analysis

The cations and anions dissolved by the chemical weathering of different rocks contribute to the combination of water in nature [52]. Therefore, the ion ratio characteristics can reflect the water–rock reaction and evolution process between natural water and rock strata [39]. As can be seen in the regional geological map (Figure 1), the main runoff areas of rivers are mainly developed strata, such as the Muganggri Group, Langshan formation, Yanshiping formation, and Nuoco formation. The lithology of these strata is principally carbonate rock, sandstone, and conglomerate.

Na^+ and K^+ are mainly derived from evaporite or silicate, and Ca^{2+} and Mg^{2+} are mainly derived from carbonate and silicate weathering and evaporative dissolution [53]. Thus, when the ratio of $\gamma(\text{Na}^+ + \text{K}^+)$ and $\gamma(\text{Cl}^-)$ is close to or above the 1:1 line, dissolution of evaporite is the leading role for Na^+ and K^+ in water chemical evolution. Figure 7a shows that the sample points of $\gamma(\text{Na}^+ + \text{K}^+)$ and $\gamma(\text{Cl}^-)$ are distributed around a straight line, with a slope of 1.63 and R^2 of 0.99. Most of the water bodies (except glaciers) are almost on the upper side of the 1:1 line, indicating that halite (NaCl) and potassium salt (KCl) are the main sources of Na^+ , K^+ , and Cl^- , and the Cl^- content is not enough to balance the content of Na^+ and K^+ in water. The excess Na^+ and K^+ may be derived from the weathering and dissolution of silicate rock.

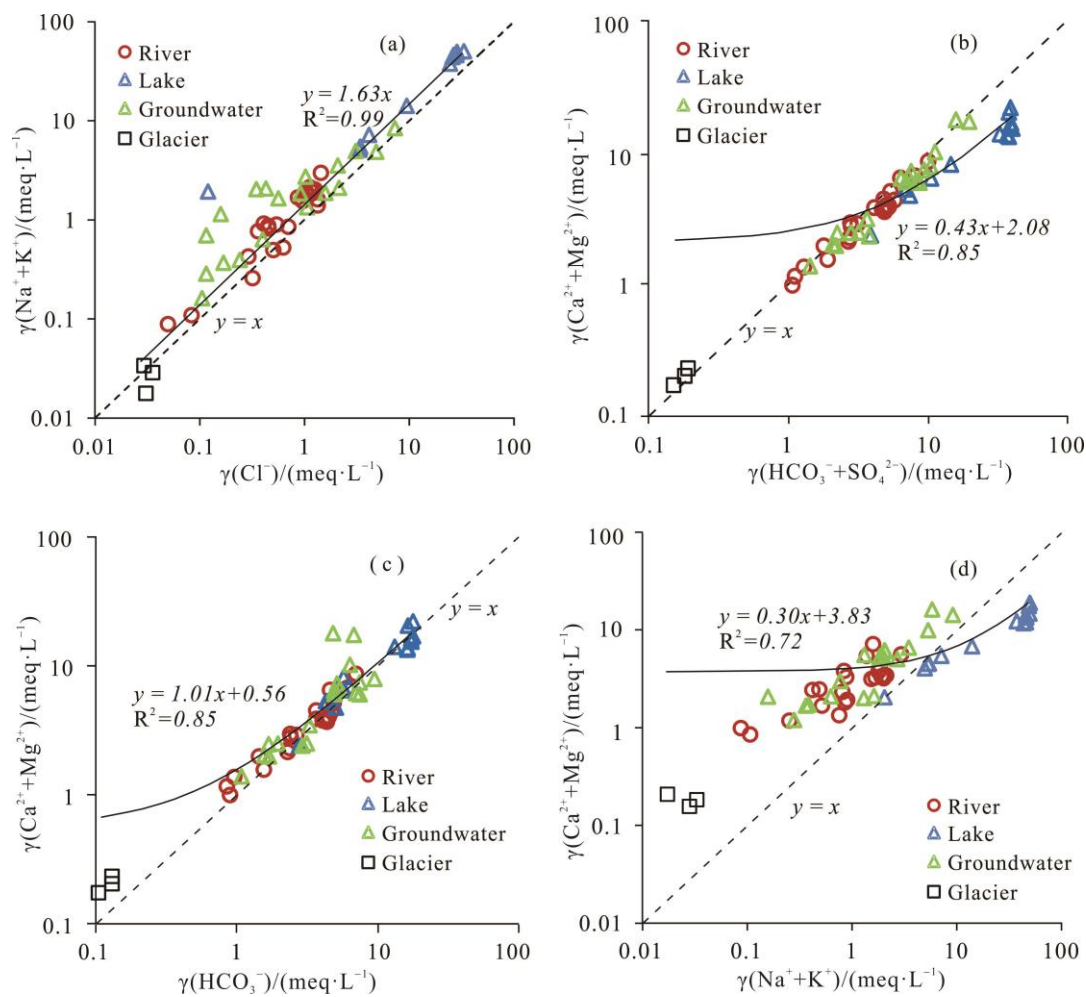


Figure 7. Distributions of ionic ratios in water samples: (a) $\gamma(\text{Na}^+ + \text{K}^+)$ versus $\gamma(\text{Cl}^-)$; (b) $\gamma(\text{Ca}^{2+} + \text{Mg}^{2+})$ versus $\gamma(\text{HCO}_3^- + \text{SO}_4^{2-})$; (c) $\gamma(\text{Ca}^{2+} + \text{Mg}^{2+})$ versus $\gamma(\text{HCO}_3^-)$; (d) $\gamma(\text{Ca}^{2+} + \text{Mg}^{2+})$ versus $\gamma(\text{Na}^+ + \text{K}^+)$.

Carbonates, evaporates, or silicates containing calcium and magnesium are the main sources of Ca^{2+} and Mg^{2+} ions in natural water [24]. Figure 7b shows the ratio of $(\text{Ca}^{2+} + \text{Mg}^{2+})$ to $(\text{HCO}_3^- + \text{SO}_4^{2-})$ in the water sample. The slope of the scattered fitting line of the water samples is 0.43, and the R^2 is 0.85, indicating that many sample points are below the 1:1 line, especially the lake points. In these water bodies, Ca^{2+} and Mg^{2+} contents are not high enough to reach equilibrium with HCO_3^- and SO_4^{2-} , and it is generally believed that the dissolution of evaporites that contain mirabilite (Na_2SO_4), polyhalite ($\text{K}_2\text{Ca}_2\text{Mg}[\text{SO}_4]_4 \cdot 2\text{H}_2\text{O}$), etc., may provide abundant SO_4^{2-} or HCO_3^- for the water bodies.

The ratio of $\gamma(\text{Ca}^{2+} + \text{Mg}^{2+})$ and $\gamma(\text{HCO}_3^-)$ can further be used to investigate the source of Ca^{2+} and Mg^{2+} [6]. As can be seen in Figure 7c, these sample points fit a line with a slope of 1.01, and the R^2 is 0.85, which is close to 1:1 line. This indicates that Ca^{2+} , Mg^{2+} , and HCO_3^- in river water, groundwater, and other water bodies are mainly derived from the dissolution of dolomite ($\text{CaMg}(\text{CO}_3)_2$) and calcite (CaCO_3) rather than gypsum (CaSO_4).

Generally, silicates are more difficult to weather than carbonates. Thus, the ratio of $(\text{Ca}^{2+} + \text{Mg}^{2+})/(\text{Na}^+ + \text{K}^+)$ or $\gamma(\text{HCO}_3^-)/\gamma(\text{Na}^+ + \text{K}^+)$ in the water can be used as a symbol for judging the main types of weathered rocks in natural water [24]. As shown in Figure 7d, there are obvious differences between lake water and other water points. The high ratios of $\gamma(\text{Ca}^{2+} + \text{Mg}^{2+})/\gamma(\text{Na}^+ + \text{K}^+)$ in the river water and groundwater indicate flow through the carbonate weathering regions (Figure 7d). Additionally, the lake samples were located

on the lower side of the 1:1 line, which confirmed that silicate dissolution or evaporate dissolution contributes to the main ion characteristics (Figure 7d).

3.2.3. Hydrochemical Modeling of Mineral Saturation Index (SI)

The saturation index (SI) of the main minerals in natural water indicates the equilibrium state between minerals and water and distinguishes the dissolution and precipitation reaction of minerals to simulate the trend of water chemistry in the environment. Phreeqc software is a hydrochemical simulation software developed by the United States District Survey, which can calculate the saturation index of minerals in groundwater. The saturation index (SI) is calculated as

$$SI = \lg \frac{IAP}{K}$$

where *IAP* is the ionic activity product, and *K* is the equilibrium constant. $SI > 0$ indicates that the mineral is saturated, and precipitate occurs. $SI = 0$ indicates that the mineral reached the equilibrium state, relatively stable. $SI < 0$ indicates that the mineral is not saturated, and a dissolution reaction occurs [51].

The ion ratio analysis of water in the study area showed that halite and carbonate minerals were the main minerals of the water–rock reaction. The solubility relationship between dolomite, calcite, and halite is shown in Figure 8. There are some differences in the saturation index (SI) of minerals in various water bodies. The salt mines have the largest halite SI, varying from -3.96 to 0.27 . The ranges of halite SI in the lake, groundwater, river water, and glaciers are -8.36 – -4.59 , -9.48 – -5.96 , -10.13 – -7.06 , and -11.07 – -10.65 , respectively. The saturation index (SI) of calcite and dolomite in the river and groundwater samples has a smaller variation and is generally within ± 1 or ± 2 , indicating that these minerals tend to be saturated continuously during the hydrochemical evolution. The ranges of calcite and dolomite SI in lake water are 0.29 – 0.87 and 0.71 – 3.17 , respectively. On the contrary, the calcite and dolomite SI values in glaciers are less than 0 and have a range of -3.3 – -2.18 and -7.41 – -4.82 , respectively.

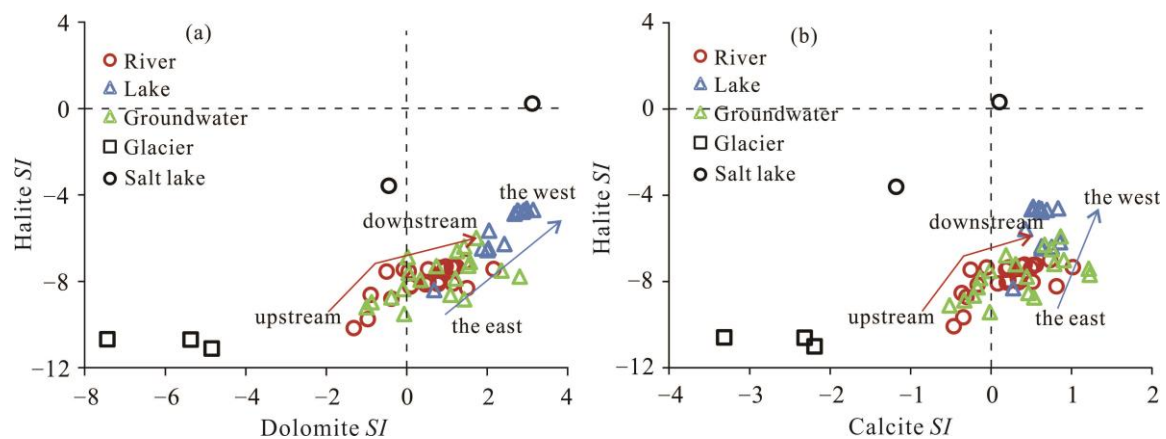


Figure 8. SI relationship between halite/dolomite (a) and halite/calcite (b) (the salt lake samples are data collected from the literature, as shown in Table 1).

The results showed that the saturation state of calcite, dolomite, and halite was not reached in glacier meltwater and upstream river water bodies. With the contact between the river and the carbonate rock strata in the flowing area, calcite and dolomite in the river bodies in the middle and lower and Bangong Co Lake water reached saturation. Overall, the halite saturation index of Bangong Co Lake showed an increasing trend from east to west, but it did not reach the saturation state like the river water. This indicates that the calcite and dolomite gradually become saturated from unsaturated to saturated, while halite dissolves during water flow from upstream to downstream and into the lake. The data collected from the salt lakes in this area show that the saturation index of calcite,

dolomite, and halite in some salt lakes is greater than 0, indicating the precipitation of calcite, dolomite, and halite.

Previous studies [35,48] pointed out that the Bangong Co Lake basin experienced a period of basin shrinkage during the plateau's uplift. During this time, some independent intermountain lakes entered the evaporite-deposition period due to abrupt regional drought climate, forming the characteristics of dispersed salt lake salt mines in the area, such as the Jieze salt mine [48] and the Taicuo salt mine [49] (Figure 1). Through the collection of chemical composition data on the salt lake water body and salt mine soil layer (Table 1), it can be seen that there are rich minerals such as halite (NaCl), dolomite ($\text{CaMg}(\text{CO}_3)_2$), calcite (CaCO_3), and mirabilite (NaSO_4) in these lacustrine chemical sedimentary profiles. Under rain erosion or lateral river water intrusion, the interlacustrine group continuously replenishes rivers and lakes, providing abundant Na^+ , K^+ , Cl^- , and SO_4^{2-} ions. Therefore, the rich carbonate strata, the rock salt minerals produced in the historical environment, and the arid climate environment in the study area lead to the diverse hydrochemical characteristics in the basin.

3.2.4. Principal Component Analysis (PCA)

Principal component analysis (PCA) can reduce the dimension of the data set by converting the original variables into new and uncorrelated variables generated by retaining original information [54]. Many studies have used the principal component analysis (PCA) technique to identify important water quality parameters [55,56]. Before component analysis, all data passed the Kaiser–Meyer–Olkin (KMO) value (0.704) and Bartlett's test of sphericity statistics ($p < 0.05$) by using Origin2022 to evaluate the feasibility of principal component analysis (PCA) for source apportionment [57].

By filtering principal components (PCs) with an eigenvalue greater than 1 [29], only two PCs were extracted from the scree plot and explained 89.0% of the total variance (Table 2 and Figure 9). K^+ , Na^+ , Mg^{2+} , HCO_3^- , Cl^- , SO_4^{2-} , TDS, As, and EC have a relatively high loading on the principal component PC1, accounting for 75.4% of the total variance. PC2 explained 13.6% of the total variance and has a strong positive loading for Ca^{2+} and NO_3^- and weak negative loading for pH. Given the water sample loading distribution (Figure 9a), the loading of lake water points in PC1 is higher than that of other water bodies. The high salinity (TDS) and other ions in lake water are mainly caused by the dry environment and the lithology of the regional strata. Therefore, PC1 mainly indicates the characteristics of natural sources. Lin, Dong, and Wang pointed out that the concentration of heavy metals, such as As, Mn, and Ni, in the water body of Bangong Co Lake was lower than the background value of the water body in Tibetan areas, indicating that those heavy metals in the water were mainly derived from natural rock weathering [29]. This also verified that PC1 containing high loadings of As and TDS in this study mainly represented natural sources. PC2 comprised Ca^{2+} , NO_3^- , and pH. According to the loading distribution of the sample points (Figure 9a), the points with high PC2 loadings are mainly groundwater and a few river water points, which are mainly located in the human living, farming area, and the valley area where the meadow grows in the alluvial fan of the Doma River. This indicates that PC2 mainly illustrates animal husbandry activities and human activities. The middle and lower reaches of the Doma River and Makazangbu River are important animal husbandry areas, agricultural irrigation areas, and human living areas, indicating that agricultural fertilization and human activities have a certain impact on the water environment.

Table 2. Loadings of each variable on principal component (PC) comparison of Bangong Co Lake Watershed.

Elements	Component	
	PC1	PC2
K ⁺	0.305	0.041
Na ⁺	0.317	0.012
Ca ²⁺	−0.081	0.676
Mg ²⁺	0.312	0.115
Cl [−]	0.317	0.034
SO ₄ ^{2−}	0.311	0.102
HCO ₃ [−]	0.300	0.172
NO ₃ [−]	−0.079	0.636
TDS	0.317	0.041
EC	0.318	0.041
TH	0.302	0.047
pH	0.182	−0.248
As	0.289	−0.126
Eigenvalue	9.801	1.767
Variance (%)	75.393	13.593

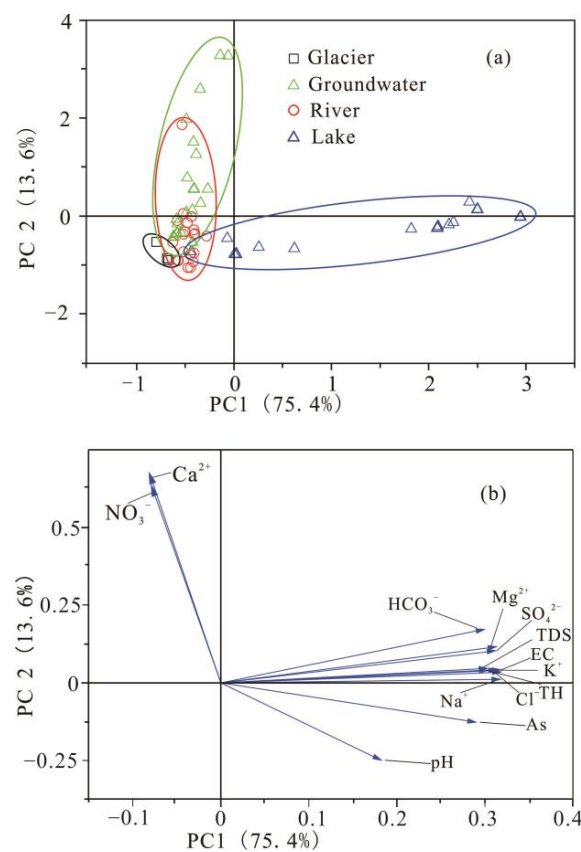


Figure 9. (a) Score plot of principal component analysis of major ions in water samples from the study area; (b) loading plot of principal component analysis of major ions in water samples from the study area.

3.3. Water Quality Evaluation

3.3.1. Assessment of Groundwater Suitability for Drinking Purposes

A drinking water quality index (DWQI) method was used to assess the suitability of groundwater for drinking [41,42]. The drinking water quality index (DWQI) is a water quality assessment method proposed by Horton RK and widely used [58]. This technique

used the weighted index method to change many water quality parameters into a single index that can be compared, effectively providing a comprehensive groundwater quality evaluation model [59]. The calculation of the drinking water quality index (DWQI) can be divided into several steps: (a) Assignment of each parameter's weight according to its relative importance (values from 2 to 5), (b) calculation of the relative weight for each index (W_i), (c) the rate calculation of the quality parameter (Q_i), and (d) the water quality index computation of each sample. These data formulas are calculated via the following equations:

$$W_i = w_i / \sum_{i=1}^n w_i$$

$$Q_i = (C_i - C_{ip}) / (S_i - C_{ip}) \times 100$$

$$DWQI = \sum(Q_i \times W_i)$$

where W_i is the relative weight, w_i is the weight of each parameter, n is the total number of parameters considered for the drinking water quality index (DWQI) calculation, and C_i is the concentration of each parameter (mg/L). C_{ip} is the ideal value of the parameter in pure water, and S_i is the standard value of each parameter.

In this study, an analysis of eleven water quality parameters, namely, pH, TH, TDS, Cl^- , SO_4^{2-} , NO_3^- , F^- , Na^+ , As, and Mn, was used to evaluate the suitability of groundwater for drinking. The relative weight of each parameter and its weight used in these calculations are presented in Table 3. Based on drinking water quality index (DWQI) values [41,51,60], the groundwater quality status can be categorized into five types: Excellent water (<20), good water (≥ 20 and <40), poor water (≥ 40 and <80), very poor water (≥ 80 and <120) and water unsuitable for drinking (≥ 120). In the Bangong Co Lake Watershed, the computed DWQI values vary from 12 to 86, with an average value of 32 ± 20 . According to the DWQI classification, 26% ($n = 5$) of the total groundwater samples fall under the excellent category, and 53% ($n = 10$) are classified as good water, respectively. About 21% ($n = 4$) of groundwater samples fell under moderate water quality (poor and very poor), and no sample was labeled as unsuitable for drinking (Figure 10). Figure 10 shows the spatial distribution of the drinking water quality index (DWQI), which illustrates that the chemical characteristics of groundwater in the lakeshore zone do not have a regular distribution in the east–west direction. Meanwhile, wells located near the lakeshore have higher drinking water quality index (DWQI) values than those away from the lakeshore, indicating that groundwater near the lakeshore may be affected by lake water (Figure 10).

Table 3. The relative weight for each index and weight assigned for drinking water quality index (DWQI).

Parameters	Weight	Relative Weight
Na^+	2	0.047
Cl^-	4	0.093
SO_4^{2-}	3	0.070
NO_3^-	5	0.116
TDS	5	0.116
pH	3	0.070
As	5	0.116
TH	3	0.070
Fe	4	0.093
Mn	4	0.093
F^-	5	0.116

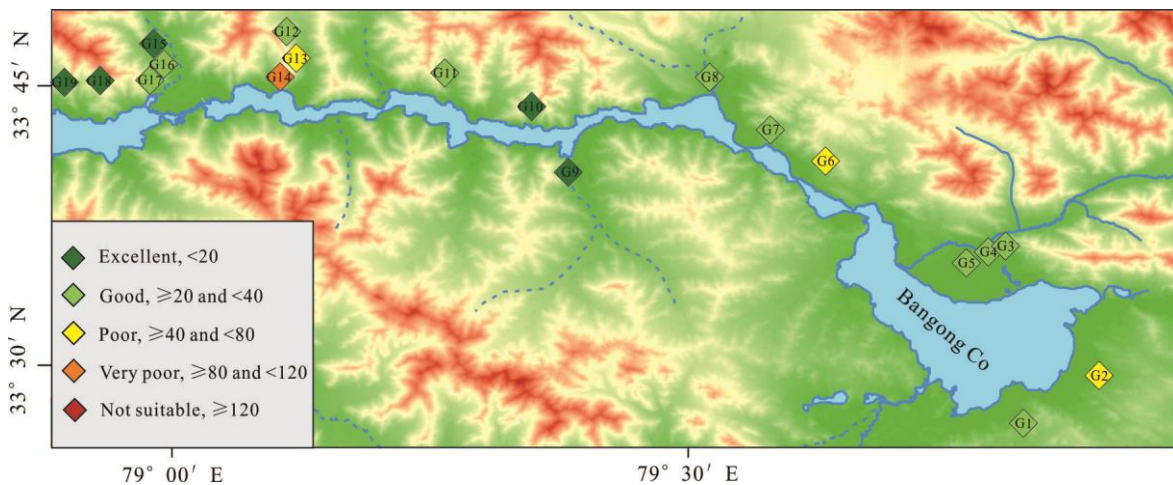


Figure 10. Assessment map of groundwater suitability in Bangong Lake Watershed.

3.3.2. Water Evaluation for Irrigation

In the plateau and semi-arid region of Bangong Co Lake Watershed, agriculture and livestock husbandry are the main occupations, and the main crops in the region are barley, rape, wheat, and peas [61,62]. Agriculture is the basic department of regional economic and social development. In addition, afforestation is an initiative advocated by the local government to improve the ecological environment [61]. Due to the fact that water quality plays an important role in crops, the survival of tree planting, and soil characteristics in the study area, groundwater irrigation suitability evaluation is necessary. To better evaluate the suitability of regional surface water and groundwater, this study uses the USSS classification proposed by Richards [43] and several other methods, such as electrical conductivity (EC), adsorption ratio (SAR), permeability index (PI), and magnesium hazardous ratio (MHR) [43,63,64]. Table 4 shows the calculation methods and sources of these parameters.

Table 4. Equations used for irrigation and irrigation water quality assessment.

IWQ Parameters and Equations	Irrigation Problem	Degree of Restriction on Use			Number of Samples (%)			Reference
		None	Slight to Moderate	Severe	None	Slight to Moderate	Severe	
EC ($\mu\text{S}/\text{cm}$)	Salinity	<700	700~3000	>3000	35 (58%)	17 (28%)	8 (13%)	[43]
$\text{SAR} = \frac{\text{Na}^+}{\sqrt{0.5 \times (\text{Ca}^{2+} + \text{Mg}^{2+})}}$	Permeability	>700	700~200	<200	51 (85%)	1 (2%)	8 (13%)	[65] [43]
$\text{PI} = \left(\frac{\text{Na}^+ + \sqrt{\text{HCO}_3^-}}{\text{Ca}^{2+} + \text{Mg}^{2+} + \text{Na}^+} \right) \times 100$		<25	25~75	>75	19 (32%)	41 (68%)	0	[63]
$\text{MHR} = \left(\frac{\text{Mg}^{2+}}{\text{Ca}^{2+} + \text{Mg}^{2+}} \right) \times 100$		<50		>50	33 (55%)	-	27 (45%)	[64]

High salinity and high sodium concentration in irrigation water are the main causes of soil salinization, which affects the growth of plants and crops [66]. The sodium adsorption ratio (SAR), recommended by Richards [43], is one of the important indices used to calculate the harm of sodium in irrigation water. In the Bangong Co Lake Watershed, the sodium adsorption ratio (SAR) value ranged from 0.03 to 16.72, with a mean value of 3.05 ± 4.92 . Based on the classification of sodium adsorption ratio (SAR) values [43,67], water samples in the Bangong Co Lake Watershed are classified into good ($n = 51, 85\%$), poor ($n = 1, 2\%$), and unsuitable ($n = 8, 13\%$). The water points with sodium adsorption ratio (SAR) values exceeding the limits are located in the west and middle parts of Bangong Co Lake. Electrical conductivity (EC), the salinity parameter of irrigation water, ranges from 23 to 7861 $\mu\text{S}/\text{cm}$ with an average value of $1493 \pm 2179 \mu\text{S}/\text{cm}$. According to electrical conductivity (EC)

value classification, water samples in the Bangong Co Lake Watershed can be classified as good ($n = 35, 58\%$), poor ($n = 17, 28\%$), and unsuitable ($n = 8, 13\%$). Similarly, the water points with severe EC values are located in the west and middle parts of Bangong Co Lake, and points with poor electrical conductivity (EC) values are mainly located in the eastern part of Bangong Co Lake and groundwater near the lake’s shoreline and lower sections of streams.

Doneen pointed out that poor soil permeability is usually caused by irrigation water with high Na^+ and HCO_3^- concentrations [63]. Thus, the permeability index (PI) is often used to evaluate the harm of a high Na ion concentration in soil in irrigation water. In this study, the permeability index (PI) ranged from 36 to 181, averaging 71 ± 26 . According to Wilcox’s classification, watershed water samples were classified as good ($n = 49, 32\%$) or suitable ($n = 41, 68\%$) [67,68].

Ayers and Westcot noticed that irrigation water with high Mg^{2+} could lead to soil Ca^{2+} deficiency and crop yield reduction [64]. In this study, the magnesium hazardous ratio (MHR) ranged from 10 to 98, with a mean of 54 ± 23 . The results show that 55% of water samples are suitable for irrigation ($\text{MHR} < 50$), and the rest of the water samples ($n = 27, 45\%$) are unsuitable ($\text{MHR} \geq 50$). The unsuitable points for irrigation of MHR are mainly the lake’s water points, some river water samples, and some groundwater samples.

The USSL classification suggested by US Salinity Laboratory Staff (1954) is a practical way to assess the suitability of irrigation water [43]. The USSL diagram best explains the combined effect of the salinity hazard and sodium hazard. In this paper, the USSL diagram (Figure 11) shows that 13% of the total samples are in the C1-S1 field, including three glacier samples, two groundwater samples, and three river samples (distributed upstream) which indicates relatively low alkalinity and salinity hazards. In the C2-S1 field, there are 10 groundwater samples, 19 river samples, and 1 lake sample with a medium of alkalinity hazard and low salinity. A total of seven groundwater samples and four lake samples (mainly in the eastern lake) are classified as part of the C3-S1 region. These samples with low sodium (S1) and low, medium, or high alkalinity (C1, C2, C3) apply to all soil types of irrigation. Only one lake sample was plotted on the C4-S2 region, and western lake samples were almost all plotted on the C5-S4 region, which is unsuitable for crops and soil irrigation. In conclusion, glacial meltwater and river water are more suitable for irrigation than lake water and some groundwater.

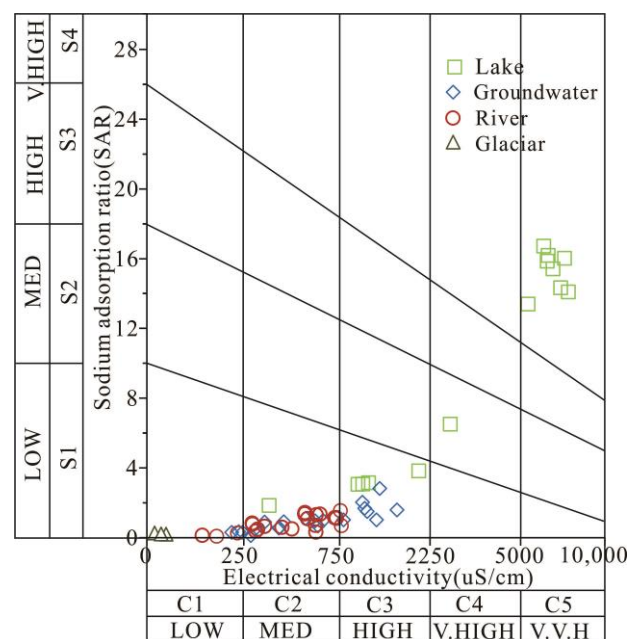


Figure 11. USSL diagram showing the suitability of groundwater for irrigation purposes.

4. Conclusions

The hydrochemical characteristics of surface water and lakeshore groundwater in Bangong Lake Watershed, Northwest Tibet, China, were analyzed using a multivariate statistical method, Piper diagrams, Gibbs diagrams, the ion ratio method, and principal component analysis (PCA). At the same time, the drinking water quality index (DWQI), irrigation water indexes, and spatial analysis were used to evaluate the quality of irrigation water and drinking water. The main conclusions are summarized below.

Most of the water samples, such as lake and river samples in the study area, were found to be slightly alkaline. Glacier water was categorized as soft-fresh, and lake water was classified as hard-brackish. Groundwater and river water were categorized as soft-fresh and hard-fresh. Na-Cl was the primary water type for lake water, while glacier, river, and groundwater were dominated by the Ca-HCO₃ type. Only 78% of groundwater samples were Ca-Cl types. The ionic concentrations of river waters showed an increased trend from upstream to downstream in terms of their spatial distribution, and high concentrations were found in the lake's coastal region. Regarding the spatial patterns of water in the Bangong Co Lake, ionic concentrations increased from east to west. There was no obvious spatial distribution of groundwater ion concentrations in the lakeshore zone in the east–west direction.

Precipitation dominance was observed in rivers and groundwater, and evaporation and crystallization dominance was observed in lakes, according to the Gibbs diagram. The ion ratio showed that the dissolution of carbonates and evaporites plays a leading role in the regional hydrochemical characteristics, corresponding to the limestone and dolomite formations widely exposed in the region. The calculation of the saturation index showed that calcite and dolomite were supersaturated in the water body of the basin, except for glaciers and some upstream rivers. Although all the lake samples from the study area were undersaturated regarding halite, their saturation index showed an increasing trend from east to west, indicating strong evaporation and continuous halite concentration characteristics. The collected data revealed salt lakes supersaturated with halite in this area. Thus, the main mineralization is related to the dissolution of calcite, dolomite, and halite in the strata. PCA showed that the regional hydrochemistry was mainly affected by natural factors, and only a few river sections and groundwater points had an anthropogenic input of NO₃[−] and Ca²⁺ plasma, which may be related to animal husbandry activities in the valley and human activities in the river sector.

Regarding drinking water quality, the drinking water quality index (DWQI) value classified the groundwater as excellent (67%), good (5%), and poor (19%). The map of the suitability assessment for drinking water demonstrated that the closer the shallow groundwater was to the lake shore, the worse the water quality. With regard to the irrigation water quality, the irrigation water indexes indicated that glaciers, rivers, most groundwater, and a small part of the east lake are suitable for irrigation, while these indicators also indicated that the west and middle lake ($n = 8$, 13%) are not suitable for irrigation. The permeability index (PI), electrical conductivity (EC), and USSS classification showed that some shallow groundwater near the lake shoreline and the lake water on the east side have moderate hazards in terms of salinity and permeability, and it is necessary to consider rational use for different types of land irrigation. Overall, the primary contribution of this research will help the Bangong Co Lake area sustainably utilize water resources.

Author Contributions: Writing—Review and Editing, Y.S. and B.Y.; Writing—Original Draft Preparation, Y.S. and L.L.; Investigation, K.G. and K.Z.; Project Administration, X.Y.; Software, G.F. All authors have read and agreed to the published version of the manuscript.

Funding: The research is sponsored by the China Geological Survey Project ([2023]10-02-01), and supported by State Key Laboratory of Loess and Quaternary Geology Open Fund (SKLLQG2241).

Data Availability Statement: The data that support the findings of this study are available from the corresponding author B.Y. upon reasonable request.

Acknowledgments: The authors gratefully acknowledge J.W. at laboratory of Xizang Shengyuan Environmental Engineering Co., Ltd. for the constant help. We also thank the contributions of H.Y., H.H., and X.Z. at Research Center of Applied Geology of China Geological Survey.

Conflicts of Interest: The authors declare no conflict of interest.

References

1. Wang, X.P.; Gong, P.; Wang, C.F.; Ren, J.; Yao, T.D. A review of current knowledge and future prospects regarding persistent organic pollutants over the Tibetan Plateau. *Sci. Total Environ.* **2016**, *573*, 139–154. [[CrossRef](#)] [[PubMed](#)]
2. Yafeng, S.; Jiawen, R. Glacier recession and lake shrinkage indicating the climatic warming and drying trend in central Asia. *Ann. Glaciol.* **1990**, *14*, 261–265. [[CrossRef](#)]
3. Yan, L.J.; Zheng, M.B.; Wei, L.J. Change of the lakes in Tibetan Plateau and its response to climate in the past forty years. *Front. Earth Sci.* **2016**, *23*, 310–323.
4. Zhang, R.; Zhu, L.; Ma, Q.; Chen, H.; Liu, C.; Zubaida, M. The consecutive lake group water storage variations and their dynamic response to climate change in the central Tibetan Plateau. *J. Hydrol.* **2021**, *601*, 126615. [[CrossRef](#)]
5. Jin, Z.D.; You, C.F.; Wang, Y.; Shi, Y. Hydrological and solute budgets of Lake Qinghai, the largest lake on the Tibetan Plateau. *Quat. Int.* **2010**, *218*, 151–156. [[CrossRef](#)]
6. Sun, M.P.; Jin, H.A. Hydrochemistry differences and causes of tectonic lakes and glacial lakes in Tibetan Plateau. *Water* **2020**, *12*, 3165. [[CrossRef](#)]
7. Ren, J.; Wang, X.; Wang, C.; Gong, P.; Yao, T. Atmospheric processes of persistent organic pollutants over a remote lake of the central Tibetan Plateau: Implications for regional cycling. *Atmos. Chem. Phys.* **2016**, *14*, 1401–1415.
8. Wang, C.; Zhou, H.; Kuang, X.; Hao, Y.; Shan, J.; Chen, J.; Li, L.; Feng, Y.; Zheng, Y. Water quality and health risk assessment of the water bodies in the Yamdrok-tso basin, southern Tibetan Plateau. *J. Environ. Manag.* **2021**, *300*, 113740. [[CrossRef](#)]
9. Zhang, Y.; Zhang, Y.; Shi, K.; Zhou, Y.; Li, N. Remote sensing estimation of water clarity for various lakes in China. *Water Res.* **2021**, *192*, 116–128. [[CrossRef](#)]
10. Li, H.; Li, J.; Liu, X.L.; Yang, X.; Zhang, W.; Wang, J.; Niu, Y.Q. Composition characteristics and source analysis of major ions in four small lake-watersheds on the Tibetan Plateau, China. *Huan Jing Ke Xue Huanjing Kexue* **2015**, *36*, 430–437.
11. Wang, P.; Shang, Y.N.; Shen, L.C. Characteristics and evolution of hydrochemical compositions of freshwater lake in Tibetan plateau. *Huan Jing Ke Xue Huanjing Kexue* **2013**, *34*, 874–881. [[PubMed](#)]
12. Gunkel, A.; Shadeed, S.; Hartmann, A.; Wagener, T.; Lange, J. Model signatures and aridity indices enhance the accuracy of water balance estimations in a data-scarce Eastern Mediterranean catchment. *J. Hydrol. Reg. Stud.* **2015**, *4*, 487–501. [[CrossRef](#)]
13. Medici, G.; Lorenzi, V.; Sbarbati, C.; Manetta, M.; Petitta, M. Structural classification, discharge statistics, and recession analysis from the springs of the Gran Sasso (Italy) carbonate aquifer; comparison with selected analogues worldwide. *Sustainability* **2023**, *15*, 10125. [[CrossRef](#)]
14. He, W.M.; Song, Y.G.; Zhang, C.S.; Zhang, Q.F. Mineral elements exchange patterns in biogeochemical cycle of Jinshuhe River Basin. *Ecol. Environ. Sci.* **2011**, *20*, 217–225.
15. Li, X.; Gao, S.; Li, W.; Qiu, G.; Tian, Z. Temporal and spatial evolution of lakes in the Bashang Plateau for nearly recent 30 years. *J. Water Resour. Prot.* **2022**, *2*, 698–708. [[CrossRef](#)]
16. Bazova, M.; Moiseenko, T. Migration activity of elements in the water of lakes of northwestern Russia. *Geochem. Int.* **2021**, *59*, 970–982. [[CrossRef](#)]
17. Baranov, D.Y.; Moiseenko, T.I.; Dinu, M.I. Geochemical trends in the formation of atmospheric precipitation in the conditionally background area of the Valdai National Park. *Geochem. Int.* **2020**, *58*, 1159–1173. [[CrossRef](#)]
18. Xiao, C.L.; Liang, X.J.; Wang, B. *Hydrogeology*, 2nd ed.; Tsinghua University Press: Beijing, China, 2010.
19. Jiang, H.C.; Lv, Q.Y.; Yang, J.; Wang, B.C.; Dong, H.L.; Gonsior, M.; Schmitt-Kopplin, P. Molecular composition of dissolved organic matter in saline lakes of the Qing-Tibetan Plateau. *Org. Geochem.* **2022**, *167*, 104400. [[CrossRef](#)]
20. Xu, H.; Hou, Z.; An, Z.; Liu, X.; Dong, J. Major ion chemistry of waters in Lake Qinghai catchments, NE Qinghai-Tibet plateau, China. *Quat. Int.* **2010**, *212*, 35–43. [[CrossRef](#)]
21. Zhu, S.; Zhang, F.; Zhang, Z.; Kung, H.-T.; Yushanjiang, A. Hydrogen and oxygen isotope composition and water quality evaluation for different water bodies in the Ebinur Lake Watershed, Northwestern China. *Water* **2019**, *11*, 2067. [[CrossRef](#)]
22. Kumar, R.; Parvaze, S.; Huda, M.; Allaie, S. The changing water quality of lakes—a case study of Dal Lake, Kashmir Valley. *Environ. Monit. Assess.* **2022**, *194*, 228. [[CrossRef](#)] [[PubMed](#)]
23. Sun, R.; Zhang, X.Q.; Wu, Y.H. Major ion chemistry of water and its controlling factors in the Yamzhog Yumco Basin, South Tibet. *J. Lake Sci.* **2012**, *24*, 600–608.
24. Guo, J.M.; Kang, S.C. Temporal and spatial variations of major ions in Nam Co Lake water, Tibetan Plateau. *Huan Jing Ke Xue Huanjing Kexue* **2012**, *33*, 2295–2302. [[PubMed](#)]
25. Fontes, J.C.; Gasse, F.; Gibert, E. Holocene environmental changes in Lake Bangong basin (Western Tibet). Part 1: Chronology and stable isotopes of carbonates of a Holocene lacustrine core. *Palaeogeogr. Palaeoclimatol. Palaeoecol.* **1996**, *120*, 25–47. [[CrossRef](#)]
26. Xiao, Y.; Xie, S.Y.; Wang, M.D.; He, Y.; Hou, J.Z. Characteristics of water temperature based on fractal and R/S Method in Bangong Co and Dagze Co. *Geol. Sci. Technol. Inf.* **2015**, *34*, 200–206.

27. Hu, M.; Wang, Y.; Du, P.; Shui, Y.; Cai, A.; Lv, C.; Bao, Y.; Li, Y.; Li, S.; Zhang, P. Tracing the sources of nitrate in the rivers and lakes of the southern areas of the Tibetan Plateau using dual nitrate isotopes. *Sci. Total Environ.* **2019**, *658*, 132–140. [[CrossRef](#)] [[PubMed](#)]
28. Wen, Z.; Zheng, M.; Xu, X.; Liu, X.; Guo, G.; He, Z. Biological and ecological features of saline lakes in northern Tibet, China. *Hydrobiologia* **2006**, *541*, 189–203. [[CrossRef](#)]
29. Lin, L.; Dong, L.; Wang, Z. Hydrochemical composition, distribution, and sources of typical organic pollutants and metals in Lake Bangong Co, Tibet. *Environ. Sci. Pollut. Res.* **2021**, *28*, 9877–9888. [[CrossRef](#)]
30. Yang, H.A.; Li, Z.Q.; Ye, B.S.; Jiao, K.Q. New result of glacier inventory in the drainage basins of the Bangong lake in china. *J. Glaciol.* **2003**, *25*, 685–691.
31. Guo, G.; Zhi, J.; Ye, B. *Regional Geological Survey of 1:250,000 Ritu County, Tibet Autonomous Region (I44C003002)*; Jiangxi Institute of Geological Survey: Nanchang, China, 2004; pp. 20–120.
32. Yin, A.; Harrison, T.M. Geologic Evolution of the Himalayan-Tibetan Orogen. *Annu. Rev. Earth Planet. Sci.* **2000**, *28*, 211–280. [[CrossRef](#)]
33. Zhao, B.; Shi, R.; Zou, H.; Chen, S.; Huang, Q.; Sun, Y.L.; Yang, J. Intra-continental boninite-series volcanic rocks from the Bangong-Nujiang Suture Zone, Central Tibet. *Lithos* **2021**, *12*, 386–387. [[CrossRef](#)]
34. Li, H.L.; Gao, C.; Li, Z.H.; Zhang, Z.; Peng, Z.M.; Guan, J.L. Age and tectonic significance of Jingzhushan Formation in Bangong Lake Area, Tibet. *Geotecton. Et Metallog.* **2016**, *40*, 663–673.
35. Liu, F.; Liu, D.; Zhou, T. Causes and Tectonic Evolution of Bangong Lake Basin. *Earth Sci. J. China Univ. Geosci.* **2013**, *38*, 745–754.
36. Li, Y.; Li, M.; Cao, Y. Cashmere Diameter Deviation Of Tibetan Cashmere Goats. *Acta Vet. Et Zootech. Sinica* **1999**, *30*, 432–437.
37. Piper, M. A graphic procedure in the geochemical interpretation of water-analyses. *Trans. Am. Geophys. Union* **1944**, *25*, 914–923. [[CrossRef](#)]
38. Gibbs, R.J. Mechanisms controlling world water chemistry. *Science* **1970**, *170*, 1088–1090. [[CrossRef](#)]
39. Meybeck, M. Global chemical weathering of surficial rocks estimated from river dissolved loads. *Am. J. Sci.* **1987**, *287*, 401–428. [[CrossRef](#)]
40. WHO. *Guidelines for Drinking-Water Quality*; Fourth Edition Incorporating the First Addendum; WHO: Geneva, Switzerland, 2017; pp. 308–475.
41. Adimalla, N.; Li, P.; Venkatayogi, S. Hydrogeochemical evaluation of groundwater quality for drinking and irrigation purposes and integrated interpretation with water quality index studies. *Environ. Process.* **2018**, *5*, 363–383. [[CrossRef](#)]
42. Sarkar, M.; Pal, S.C.; Islam, A.R.M.T. Groundwater quality assessment for safe drinking water and irrigation purposes in Malda district, Eastern India. *Environ. Earth Sci.* **2022**, *81*, 11–20. [[CrossRef](#)]
43. Richards, L.A. Diagnosis and improvement of saline and alkali soils. *Soil Sci.* **1954**, *78*, 290. [[CrossRef](#)]
44. Wu, J.; Xue, C.; Tian, R.; Wang, S. Lake water quality assessment: A case study of Shahu Lake in the semiarid loess area of northwest China. *Environ. Earth Sci.* **2017**, *76*, 232. [[CrossRef](#)]
45. Xiao, J.; Zhang, F.; Jin, Z. Spatial characteristics and controlling factors of chemical weathering of loess in the dry season in the middle Loess Plateau, China. *Hydrol. Process.* **2016**, *30*, 4855–4869. [[CrossRef](#)]
46. Kim, Y.; Mo, H.; Son, J.; Lee, Y.S.; Lee, S.E.; Cho, K. Interactive effects of water pH and hardness levels on the growth and reproduction of *Heterocypris incongruens* (Crustacea: Ostracoda). *Hydrobiologia* **2015**, *753*, 97–109. [[CrossRef](#)]
47. Ganguli, S.; Rifat, M.a.H.; Howlader, S.; Hasan, M.A.; Islam, S.; Alam, M.N.E.; Islam, M.N. Assessment of Bhatiari Lake water quality: Pollution indices, hydrochemical signatures and hydro-statistical analysis. *J. Indian Chem. Soc.* **2022**, *99*, 105–115. [[CrossRef](#)]
48. Hu, W. *Geological Characteristics and Uplifting Environment Evolution of Salt Lake in the Eastern Section of Pangong Lake in Xizang Province*; China University of Geosciences (Wuhan): Wuhan, China, 2014; pp. 1–61.
49. Liu, J.; Wei, L.; Zheng, M. Distribution and Characteristics of Carbonate and Elementary Geochemistry of Profile TT-1 in Dahyab Tso (Tai Cuo) Tibet and Its Palaeoenvironment Significance. *Acta Geol. Sin.* **2007**, *81*, 1289–1298.
50. Wang, J.Y.; Long, A.H.; Deng, M.J.; Xie, L. Water balances of east and west lakes Balkhash and their ptimization management. *J. Glaciol.* **2011**, *33*, 1353–1362.
51. Kammoun, A.; Abidi, M.; Zairi, M. Hydrochemical characteristics and groundwater quality assessment for irrigation and drinking purposes: A case of Enfidha aquifer system, Tunisia. *Environ. Earth Sci.* **2022**, *81*, 41. [[CrossRef](#)]
52. Fadili, A.; Najib, S.; Mehdi, K.; Riss, J.; Makan, A.; Boutayeb, K.; Guessir, H. Hydrochemical features and mineralization processes in coastal groundwater of Oualidia, Morocco. *J. Afr. Earth Sci.* **2016**, *116*, 233–247. [[CrossRef](#)]
53. Zhang, Y.; Zhu, G.F.; Ma, H.Y.; Yang, J.X.; Pan, H.X.; Guo, H.W.; Wan, Q.Z.; Yong, L.L. Effects of Ecological Water Conveyance on the Hydrochemistry of a Terminal Lake in an Inland River: A Case Study of Qingtu Lake in the Shiyang River Basin. *Water* **2019**, *11*, 1673. [[CrossRef](#)]
54. Gu, Y.G.; Li, Q.S.; Fang, J.H.; He, B.Y.; Fu, H.B.; Tong, Z.J. Identification of heavy metal sources in the reclaimed farmland soils of the pearl river estuary in China using a multivariate geostatistical approach. *Ecotoxicol. Environ. Saf.* **2014**, *105*, 7–12. [[CrossRef](#)]
55. Ahmad, S.; Singh, N.; Mazhar, S.N. Hydrochemical characteristics of the groundwater in Trans-Yamuna Alluvial aquifer, Palwal District, Haryana, India. *Appl. Water Sci.* **2020**, *10*, 75. [[CrossRef](#)]
56. Şehnaz, Ş.; Şener, E.; Davraz, A.; Varol, S. Hydrogeological and hydrochemical investigation in the Burdur Saline Lake Basin, southwest Turkey. *Geochemistry* **2019**, *80*, 125–135. [[CrossRef](#)]

57. Wang, D.; Shi, L. Source identification of mine water inrush: A discussion on the application of hydrochemical method. *Arab. J. Geosci.* **2019**, *12*, 121–134. [[CrossRef](#)]
58. Horton, R.K. An index number system for rating water quality. *J. Water Pollut. Control Fed.* **1965**, *37*, 300–306.
59. Ali, Z.I.; Gharbi, A.; Zairi, M. Evaluation of groundwater quality in intensive irrigated zone of Northeastern Tunisia. *Groundw. Sustain. Dev.* **2020**, *11*, 100482.
60. Kumari, M.; Rai, S.C. Hydrogeochemical evaluation of groundwater quality for drinking and irrigation purposes using water quality index in semi arid region of India. *J. Geol. Soc. India* **2020**, *95*, 159–168. [[CrossRef](#)]
61. Yan, J.H. 2022 Government Work Report of Ali Prefecture, Tibet Autonomous Region; Tibet Daily: Lhasa, China, 2022; pp. 1–2.
62. Huntington, E. Pangong: A glacial lake in the Tibetan Plateau. *J. Geol.* **1906**, *14*, 599–617. [[CrossRef](#)]
63. Doneen, L.D. *Water Quality for Agriculture, Department of Irrigation*; University of California: Davis, CA, USA, 1964; pp. 5–10.
64. Ayers, R.S.; Westcot, D.W. *Water Quality for Agriculture*; Food and Agriculture Organization of The United Nations: Rome, Italy, 1976.
65. Bouwer, H. *Groundwater hydrology (McGraw-Hill Series in Water Resources and Environmental Engineering Series; McGraw-Hill College: New York, NY, USA, 1978; pp. 1–10.*
66. Rajmohan, N.; Masoud, M.H.Z.; Niyazi, B.a.M. Assessment of groundwater quality and associated health risk in the arid environment, Western Saudi Arabia. *Environ. Sci. Pollut. Res.* **2021**, *28*, 9628–9646. [[CrossRef](#)]
67. Wilcox, L. *Classification and Use of Irrigation Waters*; United States Department of Agriculture: Washington, DC, USA, 1955; pp. 1–5.
68. Saleh, A.; Al-Ruwaih, F.; Shehata, M. Hydrogeochemical processes operating within the main aquifers of Kuwait. *J. Arid Environ.* **1999**, *42*, 195–209. [[CrossRef](#)]

Disclaimer/Publisher’s Note: The statements, opinions and data contained in all publications are solely those of the individual author(s) and contributor(s) and not of MDPI and/or the editor(s). MDPI and/or the editor(s) disclaim responsibility for any injury to people or property resulting from any ideas, methods, instructions or products referred to in the content.